Journal of Physics:
Conference Series

PAPER • OPEN ACCESS

Characterisation of hydrophobic surfaces by droplet impact

To cite this article: Amedeo Amoresano and Silvia Roscioli 2024 *J. Phys.: Conf. Ser.* **2802** 012004

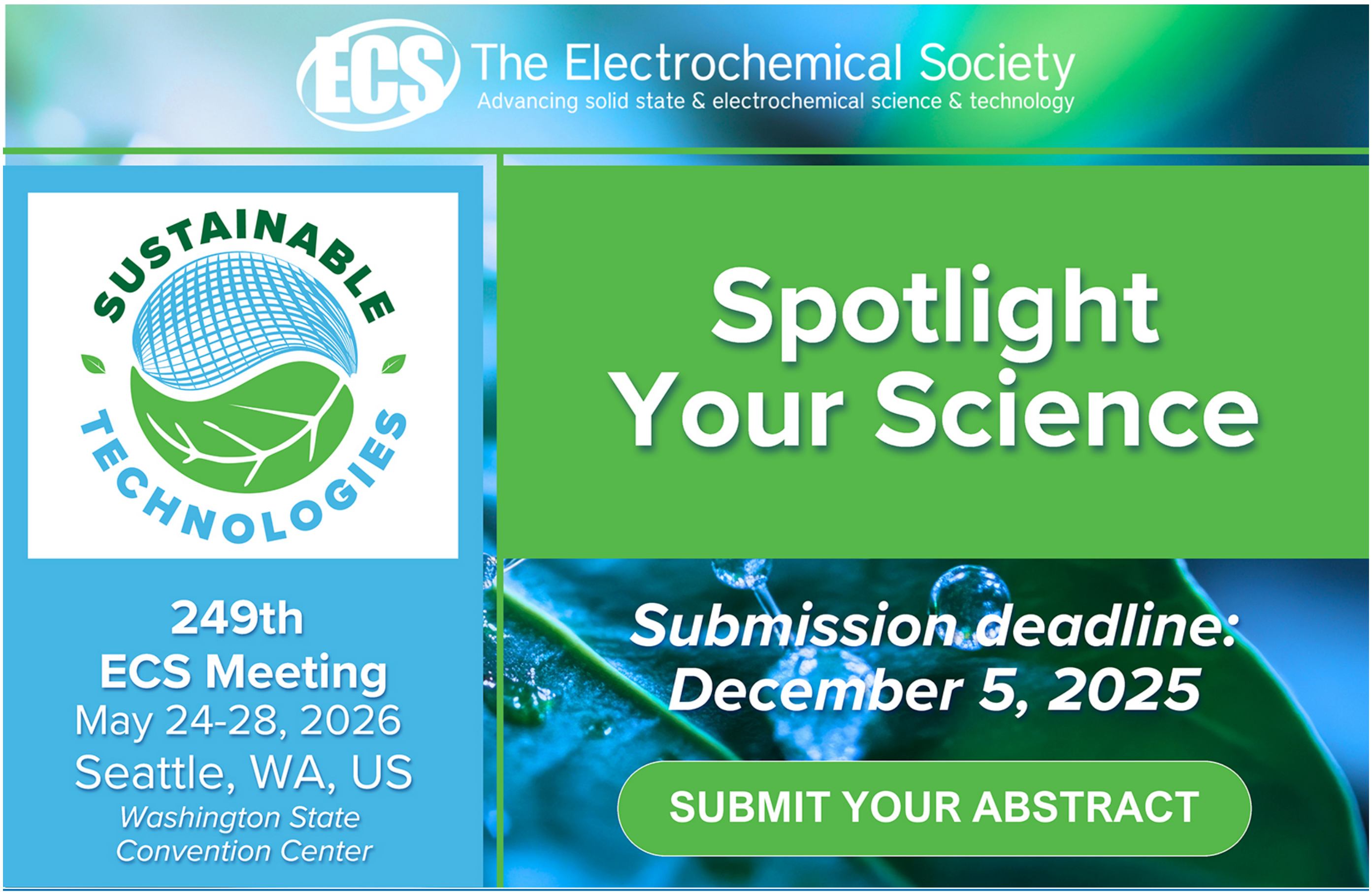

Journal of Physics: Conference Series **2802** (2024) 012004 doi:10.1088/1742-6596/2802/1/012004

Characterisation of hydrophobic surfaces by droplet impact

Amedeo Amoresano[1*], Silvia Roscioli[1]

[1] Industrial Engineering Department, University of Naples "Federico II", Naples, Italy

*E-mail: amedeo.amoresano@unina.it, ORCID ID: 0000-0003-3351-7228

Abstract. The paint industry constitutes a fundamental part of the entire industrial landscape. The primary role of paint is to preserve and protect a product from external sources such as weathering, vegetation, and rust. The maritime sector is particularly sensitive to this issue, as fouling on the hull can lead to a 40% increase in resistance, resulting in higher fuel consumption and the potential transportation of invasive species from one ecosystem to another. Paints used for ships have the characteristic of releasing biocides, primarily represented by copper and zinc, inhibiting life forms from adhering to the hull but at the same time causing a gradual "poisoning" of the ecosystem. For these reasons, new types of paints that exploit the principle of anti-adhesion rather than the release of biocides are being studied. This paper presents and characterizes epoxy-based surfaces with EPO-TQ, HDTMS, and PFOTES through experimental tests. Laboratory tests have highlighted the hydrophobicity level of each surface by evaluating the recovery time of a droplet impacting it and the final wetting angle. It has been demonstrated that among the three, the PFTOS surface exhibits the best performance and has the potential to be used as a surface/paint for naval vessels.

1. Introduction

The paint industry constitutes a fundamental part of the entire industrial landscape. The primary role of paint is to preserve and protect a product from external sources. The maritime sector is particularly sensitive to this issue, as in the water, marine organisms, plants and microorganisms attach to the surface of ship bottom and cause fouling on the hull. Micro-fouling organisms increased the friction resistance of the hull by 1%~2%. Soft fouling organisms increase the friction resistance of the hull by 10%; hard fouling organisms increase the friction resistance of the hull by 40% [1] with a consequent increase in fuel consumption, approximately equivalent to 3% [2]. This entails not only an inevitable increase in transportation costs but also a rise in terms of pollutant emissions, particularly concerning SO_x and NO_x, which are the main character both in production and regulatory terms. Additionally, there is an uptick in CO_2 production, the primary greenhouse gas.

In addition, in order to safeguard ecosystems, it is important not to transport species that are invasive and detrimental to the local marine environment, that could be very sensitive, as the artic and Antarctica areas [3].

For all these reasons, antifouling paints are using for ships. There are two main classes of anti-fouling coatings utilised by the maritime industry: biocidal anti-fouling coatings and non-biocidal foul release coatings. Both types of coating aim to delay/prevent the adhesion or the persistence of biofouling organisms on submerged surfaces [4]. Biocidal anti-fouling are released into the aquatic environments also affecting several nontarget organisms and, thus, compromising ecosystems [5]. Non-biocidal coatings are less used than the other one [4], and

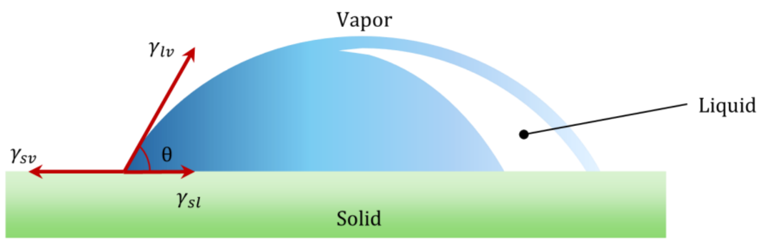

Figure 1. Surface tensions solid/vapor (γ_{sv}), solid/liquid (γ_{sl}) and liquid/vapor (γ_{lv}), and generic CA θ

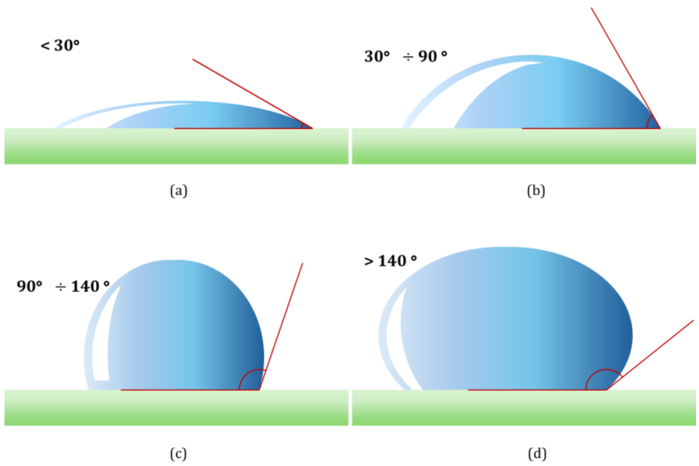

Figure 2. Different CA of drops for the surface characterisation

primarily leverage the principle of preventing fouling adhesion or weakening it against the action of water on the hull during movement. The study described in this article is precisely situated within this context. Three epoxy-based surfaces with acetone and hybrid titania (EPO-TQ), with a silicon-based silane binder (hexadecyltrimethoxysilane, HDTMS), and with a fluorine-based silane binder (1H,1H,2H,2H-perfluorooctyltriethoxysilane, PFOTES) have been studied and characterised through experimental tests. In particular, a droplet of fresh water has been dropped from three different heights onto the aforementioned surfaces to assess their level of hydrophobicity. The Contact Angle (CA) between the droplet and the surface under examination has been measured, as well as the change in droplet diameter over time until shape recovery, coalescence, or edge rupture occurred. These tests can help determine whether the material under examination is suitable for use as a coating for ships, based on its degree of non-wettability.

2. Surface wettability

Wettability is the ability of a liquid to maintain contact with a solid surface and is characterized by the contact angle between the droplet and the surface itself [6] described by the Young equation [7]:

$$\gamma_{sv} - \gamma_{sl} = \gamma_{lv}\, cos\theta$$

where γ_{sv}, γ_{sl} and γ_{lv} are the surface tensions solid/vapor, solid/liquid and liquid/vapor respectively, shown in Figure 1, and θ contact angle (CA), shown in Figure 1 and Figure 2. The wettability of the liquid-solid interface depends on the surface tension, characterized by the contact angle (CA) θ. A low value of surface tension indicates a surface with poor wettability, hence hydrophobic, while a high value represents a surface with high wettability, thus hydrophilic. In terms of CA, hydrophilic surfaces are characterized by relatively low contact angles, between 30° and 90° (Figure 2a and b), while hydrophobic ones are characterized by contact angles greater than or equal to 90° (Figure 2c), and superhydrophobic ones by contact angles greater than 140° (Figure 2d) [8]. To determine the hydrophobicity of the surfaces in question, the determination of the contact angle is one of the main objectives of the experimental tests, along with the measurement of the droplet recovery time after impact with the surface.

3. Surface characterisation

The surfaces involved in the experimental tests all share the characteristic of being based on an epoxy matrix. Each of these has been modified with a different element, namely with acetone and hybrid titania (EPO-TQ, Figure 3a), with a silicon-based silane binder (hexadecyltrimethoxysilane, HDTMS, Figure 3b), and with a fluorine-based silane binder (1H,1H,2H,2H-perfluorooctyltriethoxysilane, PFOTES, Figure 3c).

(a) (b) (c)

Figure 3. Surfaces involves in the experimental tests with: (a) EPO-TQ; (b) HDTMS; (c) PFOTES.

3.1 Experimental tests

The tests aim to calculate the CA of the droplet on the three surfaces and the variation over time of the impact and recovery diameters. The diameter variation was evaluated at three different droplet drop heights, namely 50 cm, 70 cm, and 95 cm, in order to observe the behaviour of the droplet as the kinetic energy that characterizes it changes.

The experimental setup used for the tests is shown in Figure 4 and schematically represented in Figure 5. A photographic environment was reproduced to allow automatic video recording of a sessile drop falling. In particular, as the drop passes through the LASER, the Trigger signal controlled by the photodiode is activated. The signal is processed by the FastCam Photron UX100 high-speed camera which immediately starts recording. This is transmitted through an

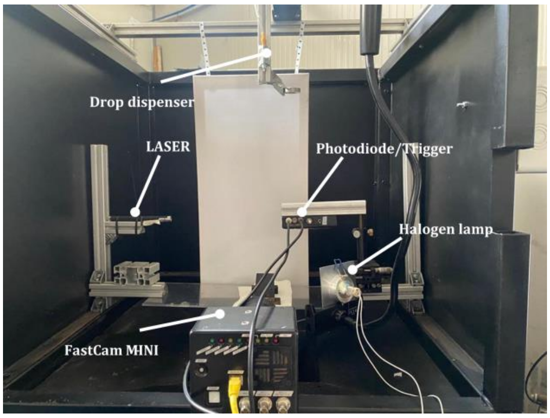

Figure 4. Experimental setup

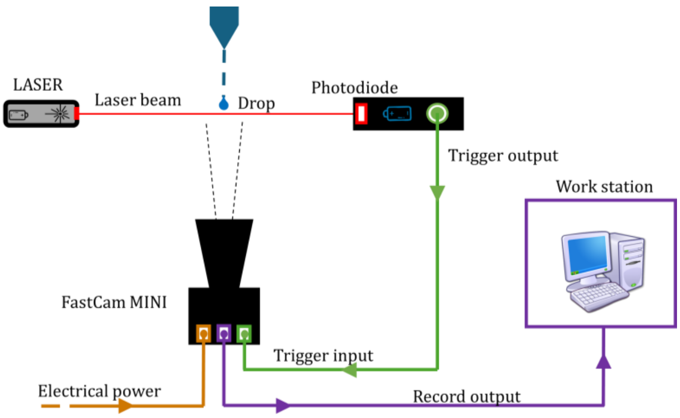

Figure 5. Scheme of plant

ethernet cable to the workstation, where the PFV4 is running. On the camera, a Canon 50 mm lens has been mounted, which allowed for an image with shallow depth of field yet stable.

To ensure adequate recording, the measurement space was illuminated using a halogen lamp HLX 64627 - OSRAM 12 V 100 W. The use of a strong light source was necessary due to the reduction in light caused by the shutter speed, which decreases as the frame acquisition frequency increases. This Xenon lamp provides light with a wavelength of approximately 650 nm, at which the Fastcam Photron UX100 sensor is particularly stable and sensitive.

3.2 Results

The contact angle has been assessed for an impacting droplet on each of the three surfaces for the three different height values. Using the PFV4 software, it has been possible to determine the droplet CA for each case once it regains its shape after impact. The results obtained are shown in Table 1.

From the results, it can be deduced that only the surface treated with PFOTES, the fluoro-based additive (**Errore. L'origine riferimento non è stata trovata.**c), exhibits hydrophobic

Table 1. Contact Angle (CA) after the shape recovery for different drop heights and surfaces.

Height	EPO-TQ	HDTMS	PFOTES
50 cm	13°	60°	66°÷93°
70 cm	13°	75°	90°÷98°
95 cm	24°	50°÷80°	103°÷110°

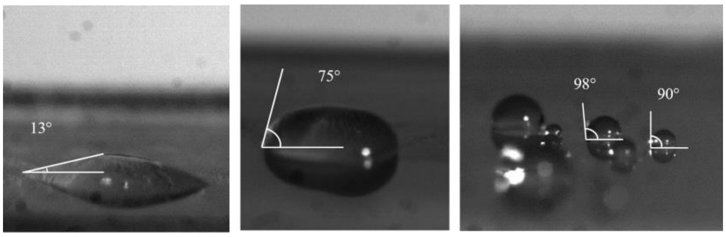

(a) (b) (c)

Figure 6. CA of droplets after shape recovery for a drop height of 70 cm for the surfaces with:
(a) EPO-TQ; (b) HDTMS; (c) PFOTES

behaviour for all test heights. Indeed, due to a CA greater than 90°, it is possible to establish that the cohesive force of water droplets is greater than the adhesion force between them and the surface. In addition, for all the values of CA for PFOTES, two values has been written. They indicate the minimum and maximum value of CA for the specific experimental test. Indeed, for all heights, after the impact with the surface and reaching a maximum extension diameter, during the rapid recovery of its shape, the surface tension was such that it completely broke the fluid film and generated, in the end, multiple droplets.

For the surfaces with EPO-TQ additive (**Errore. L'origine riferimento non è stata trovata.**a.) and HDTMS additive (**Errore. L'origine riferimento non è stata trovata.**b.), CAs are less than 90°; this makes the two surfaces in question wettable, not hydrophobic. Also, for the greater drop height of 95 cm, for the HDTMS surface, the liquid film breaks with the consequent formation of multiple droplets.

To further validate the results, the internal diameter values in pixels over time have been schematically represented for the different drop heights and materials. This allows describing the shape recovery trend of the droplet and thus characterizing the surface tension concerning the three materials. The relative time considered takes into account the moment when the droplet begins to impact until its shape stabilizes, if possible. In Figure 7a, the results obtained for a drop height of 50 cm are shown. The droplet increases in diameter until reaching a maximum extension peak, after which a shape recovery begin. What is observed for all three materials studied is consistent with what has already been defined by the contact angles. For the EPO-TQ material, indeed, the maximum extension diameter values are reached upon impact, indicating the greater adhesion force between the surface and the water particles, and the recovery diameter characterizes a coalescing droplet. The droplet has reached the stability at 0.18848 s. A complete recovery, albeit with a characteristic contact angle of a non-hydrophobic surface, is only observed for the HDTMS surface at 0.0672 s. For the fluoro-based

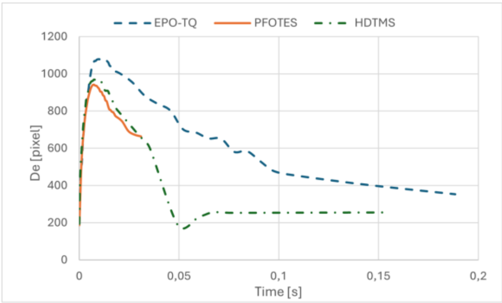

(a)

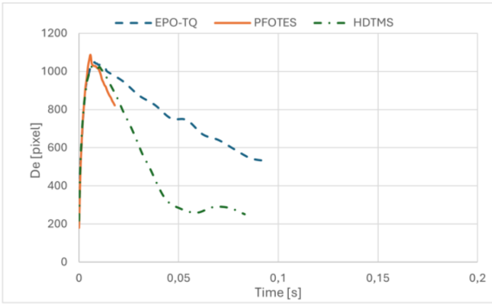

(b)

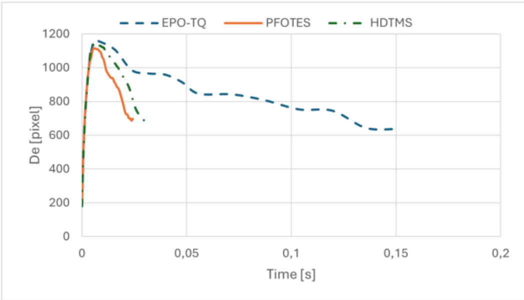

(c)

Figure 7. Trends of external diameter De for drop height 50 cm (a), 70 cm (b) and 95 cm (c)

surface, the last results recorded for this graph relate to the external diameter values until the circular crown of the droplet breaks at 0.03104 s. From that moment onwards, many droplets form on the surface, which, in addition to the contact angle values of the formed droplets, demonstrates the hydrophobic nature of the surface.

In Figure 7b, the results obtained for a drop height of 70 cm are reported. For the EPO-TQ surface, the graph shows that the trend is rather similar to that described previously. The two trends differ in the maximum diameter reached which is lower than for the 50 cm height. A beginning of coalescence is observed, indicating a surface still wettable, which slows down the recovery speed. The stability of the shape has been reached at 0.09408 s, with a diameter bigger than previously case. For the HDTMS material, the droplet reaches larger maximum diameters compared to the 50 cm height. The recovery speed is quite similar, and stability is achieved at 0.0832 seconds. For the surface treated with PFOTES, an initial rupture of the liquid film followed by the breakage of the outer circular crown can still be observed, and the recovery speed is higher both compared to the previous surfaces and to that recorded for the 50 cm height. In this case, the edge breakage occurs at 0.01792 s.

Finally, in Figure 7c, the values obtained for the impact height of 95 cm are reported. The behavior of the EPO-TQ surface remains consistent with what has been described so far, with an increase in the maximum impact diameter and shape stability at 0.15168 s. For the fluoro-based surface, once again, the rupture of the liquid film into multiple droplets is observed, at 0.02432 s. a different behaviour is shown for the HDTMS surface. The trend in this case is similarly to a hydrophobic surface. Indeed, the kinetic energy of the droplet is such that it breaks the liquid film at 0.03216 s.

4. Conclusions

The paint industry is an integral component of the overall industrial environment. The main role of paint is to preserve and protect a product from external sources such as weathering, vegetation, and rust. The paints employed on ships possess the feature of emitting biocides, predominantly comprising copper and zinc, which prevent organisms from attaching to the hull but also result in a gradual contamination of the ecosystem. For these reasons, new types of paints that exploit the principle of anti-adhesion rather than the release of have been investigated in this paper. Epoxy-based surfaces with EPO-TQ, HDTMS, and PFOTES have been studied through experimental tests in this work in order to determine the hydrophobicity degree. The experiments aim to determine the contact angle (CA) of the droplet on the three surfaces and to assess the changes over time in the impact and recovery diameters. Diameter variation was assessed at three different heights of droplet drop: 50 cm, 70 cm, and 95 cm. This has been done to observe how the droplet's behaviour changes as its kinetic energy varies. In particular, the experimental tests highlight how the tensile state of the surfaces governs the phenomenon of spreading and shape recovery of the droplets. Surfaces with low wettability tend to quickly recover the initial shape of the droplets, on condition that the energy absorbed by the droplet is not enough to cause its rupture.

The analysis have highlighted that the fluorine-based surface (PFOTES) is the only one to be completely hydrophobic, as it consistently exhibits a contact angle greater than 90° and a tendency to fragment despite low energetic values (minimum drop height) and small recovery times, unless breakage occurs, making it the most hydrophobic of the surfaces analysed. The surface treated with HDTMS exhibits good hydrophobic parameters, particularly concerning the high recovery speed, but it shows a reduced contact angle and lacks the tendency to break. Finally, the surface with EPO-TQ returned unsatisfactory results, making it the least suitable for use.

References

[1] X. Mao, X. Cui, e S. Chen, «Research Progress of Nanomaterials in the Prevention of Biological Fouling on Ships», *J. Phys. Conf. Ser.*, vol. 2002, fasc. 1, p. 012013, ago. 2021, doi: 10.1088/1742-6596/2002/1/012013.

[2] D. S. Sanz, S. García, A. Trueba, L. M. Vega, L. Trueba-Castañeda, e D. Boullosa-Falces, «Application of ceramic coatings to minimize the frictional drag penalty on ships», in *OCEANS 2021: San Diego – Porto*, set. 2021, pp. 1–5. doi: 10.23919/OCEANS44145.2021.9706045.

[3] F. T. Chan, D. Ogilvie, F. Sylvester, e S. A. Bailey, «Ship Biofouling as a Vector for Non-indigenous Aquatic Species to Canadian Arctic Coastal Ecosystems: A Survey and Modeling-Based Assessment», *Front. Mar. Sci.*, vol. 9, feb. 2022, doi: 10.3389/fmars.2022.808055.

[4] E. Arndt *et al.*, «Factors that influence vessel biofouling and its prevention and management», Final report for CEBRA Project 190803, 2021, handle link: https://hdl.handle.net/1959.11/30833 .

[5] C. A. Paz-Villarraga, Í. B. Castro, e G. Fillmann, «Biocides in antifouling paint formulations currently registered for use», *Environ. Sci. Pollut. Res.*, vol. 29, fasc. 20, pp. 30090–30101, apr. 2022, doi: 10.1007/s11356-021-17662-5.

[6] H. Hu, L. Gao, e Y. Liu, «Chapter 6 - Hydro-/ice-phobic coatings and materials for wind turbine icing mitigation», in *Wind Turbine Icing Physics and Anti-/De-icing Technology*, H. Hu, L. Gao, e Y. Liu, A c. di, in Wind Energy Engineering, Academic Press, 2022, pp. 135–168. doi: 10.1016/B978-0-12-824532-3.00500-3.

[7] F. Pochylý, S. Fialová, V. Habán, e L. Rinka, «THE WETTABILITY OF THE LIQUID-SOLID ITERFACE».

[8] J. Passaro *et al.*, «Hybrid Hemp Particles as Functional Fillers for the Manufacturing of Hydrophobic and Anti-icing Epoxy Composite Coatings», *ACS Omega*, vol. 8, fasc. 26, pp. 23596–23606, lug. 2023, doi: 10.1021/acsomega.3c01415.